PHYSICS AND CHEMISTRY OF SOLID STATE
V. 23, No. 2 (2022) pp. 256-260
Section: Physics

DOI: 10.15330/pcss.23.2.256-260

Vasyl Stefanyk Precarpathian National University

ФІЗИКА І ХІМІЯ ТВЕРДОГО ТІЛА
Т. 23, № 2 (2022) С. 256-260
Фізико-математичні науки

PACS: 81.05.ue; 81.05.uf ISSN 1729-4428

R.G. Abaszade[1], A.G. Mamedov[1], I.Y.Bayramov[1], E.A.Khanmamadova[1], V.O. Kotsyubynsky[2], O.A. Kapush[3], V.M. Boychuk[2], E.Y. Gur[4]

Structural and Electrical Properties of the Sulfur-Doped Graphene Oxide/Graphite Oxide Nanocomposite

[1]*Azerbaijan State Oil and Industry University, 16/21 Azadlıq prosp., Baku, Azerbaijan, abaszada@gmail.com*
[2]*Vasyl Stefanyk Precarpathian National University, Ivano-Frankivsk, Ukraine, kotsuybynsky@gmail.com*
[3]*V.E. Lashkarev Institute of Semiconductor Physics, NASU, Kyiv, Ukraine savchuk-olja@ukr.net*
[4]*Ataturk University, Erzurum 25240, Turkey, emregur@atauni.edu.tr*

The sulfur-doped graphene oxide/graphite oxide composite material was synthesized in an original way, and a detailed study of its structural arrangement was carried out using XRD and Raman spectroscopy. Negative differential resistive properties of the obtained material were observed on the current-voltage curve at room temperature as a result of limited proton hopping through water molecules adsorbed on the hydrophilic surface of graphene oxide layers in the presence of a sulfur-enriched graphite oxide component with high electron conductivity, which promotes spatial charge separation and increases the efficiency of H^+ transport. The obtained result offers a new way for the one-pot synthesis of new graphene-based composite materials with a wide range of possible applications.

Keywords: graphene oxide, graphite oxide, nanocomposite, negative differential resistance.

Received 17 March 2022; Accepted 10 May 2022.

Introduction

The rapid development of nanoelectronics is based on the latest achievements in material science, including graphene based materials [1; 2; 3; 4]. Graphene oxide (GO) allows the formation of large thin transparent films to replace ITO conductors in solar panels, creating new biomedical applications and microwave absorbers for electromagnetic interference [5]. It is known that the properties of carbon-based nanostructures can be controlled by doping with both metal and non-metal ions [6].

The effect of negative differential resistance (NDR) has attracted much attention due to the possibility of its application in a wide range of nanoelectronic devises, including not only resonant-tunneling diodes, high-frequency multipliers in the THz range [7, 8]. The NDR behavior has been experimentally observed in graphene [9] and graphene-based materials [10]. At the same time, the development of new technologically simple and accessible NDR materials is an important task of applied materials science. Graphene oxide and reduced graphene oxide have significant prospects as materials with voltage controlled negative differential resistance that can be used in low-power and high-speed devices [11]. Significant NDC properties found earlier at room temperature for sulfur doped graphene oxide (GO/sulfur) demonstrate [7] that it is of considerable interest for the obtaining new functional materials for nanoelectronics.

The aim of this work is a comparative study of the structural, morphological, and electrical properties of graphene oxide/graphite oxide composites synthesized by the chemical oxidation of graphite with sulfur acids.

I. Experimental details

The synthesis process can be described as follows: 10 ml of 96 % solid sulfuric acid is added to a beaker; 1 g of highly dispersed graphite (purity 99.9995 %) is

mechanically poured into 0.5 g of sodium hydroxide in the well of a Petri dish and over solid sulfuric acid. The remaining amount (13 g) is added to the system with a magnetic stirrer, adding solid sulfuric acid. Potassium permanganate (3 g) is added to the system in portions over 2 hours. During this period, the mixture comes into contact with an ice bath and the temperature is maintained at 20 degrees. After mixing is stopped, the system comes into contact with the steam of a hot water bath. This time the temperature is maintained at 35 degrees. Thus, the mixture is obtained in the form of a chestnut-gray paste. 46 ml of distilled water is added to the mixture. Immediately put to boil in a boiling water bath. After 1 hour, mix by adding 250 ml of distilled water. After a while, 100 ml of perhydrol are added and mixed. There is a change in color. Thus, the formation of a yellowish compound in chestnuts visually proves the production of graphene oxide. The mixture is filtered after lowering the temperature. The remaining substance on the filter paper is washed with distilled water. The product was dried at 50°C for 2 hours under vacuum. The weight loss of the obtained material after complete drying was about 40 %, which corresponds to [12].

X-ray diffraction phase analysis was performed on an XRD-7000 diffractometer (Shimadzu) using CuK_α radiation with 2θ scanning from 10° to 70° 2° per minute with a step of 0.02°. The Raman spectra were measured on a T64000 Jobin-Yvon spectrometer (1800/mm, resolution about 1 cm^{-1}) in inverse dispersion geometry using an argon-krypton laser (λ = 532 nm). The laser irradiation power was less than 1 mW/cm^2, which made it possible to avoid local overheating of the samples. SEM analysis was carried out using a Scanning Electron Microscope by JEOL (Oxford Instruments, 15 kV SEI, WD of 4.5 mm). Samples for electrical testing were cut in the form of rectangles and placed on a Teflon substrate. Silver paste contacts were applied to the substrate for attaching the wires so that resistance could be measured using the usual two-prong method. Volt-ampere characteristics were measured at room temperature.

II. Results and discussion

XRD patterns of the obtained materials demonstrate the presence of different phases and are fitted using the OriginPro 8.5 program with four Lorentzian functions (Fig. 1). Intense peaks at 2θ of about 9.75° correspond to the (001) reflex of graphene oxide. The calculated value of the interplanar distance $d_{(001)}$ perpendicular to the basal plane of the graphene packages is 0.888 nm.

The Scherrer equation was used to estimate the average package size *D* in the direction perpendicular to the (001) plane using the analysis of the position of the reflex (2θ, rad) and its full width at half maximum (β, rad): $D = \frac{K\lambda}{\beta cos\theta}$, where K = 0.89. The calculated value of $D_{(001)}$ was about 11.11 nm, which corresponds to an average number N of graphene layers in a package of 13 - 14. A broad peak in the range 2θ = 12 - 40°, observed on XRD patterns, corresponds to (002) reflexes of the structure of

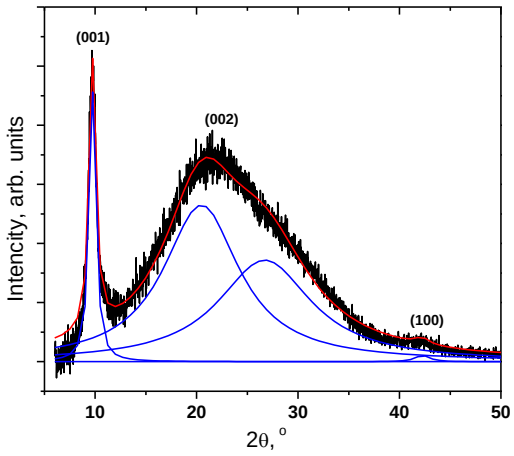

Fig. 1. XRD patterns of the synthesized graphene oxide/graphite oxide composite materials with the results of deconvolution.

a distorted graphite oxide lattice (Fig.1, a). It was optimally fitted with two sub-peaks, each of which allows one to calculate the most probable values of $d_{(002)}$ and *D* for two fractions of graphite oxide. The first (Component 1) has maxima at 2θ = 26.7, which is very close to the properties of the microcrystalline structure of graphite ($d^{(1)}_{(200)}$ = 0.335 nm) and corresponds to $D^{(1)}_{(200)}$ value of 0.646 nm. The average number of layers N is only 3, and these values rather correspond to the sizes of coherently scattered regions of incompletely exfoliated graphite. Component 2 has maxima at 2θ = 20.59°, which corresponds to $d^{(2)}_{(200)}$=0.431 nm, and for $D^{(2)}_{(200)}$=1.025, calculated value of N is 3 - 4. This value is consistent with characteristics of Component 1, and the formation of Component 2 can be explained by the relaxation of the crystal structure of coherently scattered fragments of graphite oxide after exfoliation from microcrystalline graphite particles. The last observed component of XRD pattern at 2θ = 20.59° corresponds to the two dimensional (10) reflection of the graphene oxide structure. To analyze this peak, the Scherrer equation with the Warren constant K = 1.84 was applied in accordance with [13] and the average lateral size of the GO stacking layers $L_{(10)}$ = 10.3 nm was calculated. According to the analysis of the integral intensity of the deconvoluted components, the relative content of graphene oxide in the graphite oxide/ graphene oxide mixture is about 15 - 16 %.

Independent information about the structural arrangement of the obtained materials was obtained by Raman spectroscopy.

The Raman spectra of the resulting composite (Fig. 2a) exhibit a characteristic first-order G-mode at 1561 cm^{-1}, formed as a result of in-plane stretching vibration of sp^2-bonded carbon atoms corresponding to E_{2g} optical phonons, as well as a "defect" D band about 1322 cm^{-1} (weak), which is the result of graphite disordering. The high intensity of the D band indicates structural defects in the obtained carbon material. The ratio of the integral intensities of the D and G bands (I_D / I_G) is inversely proportional to the size of graphite oxide crystallite in the basal (002) plane [14]:

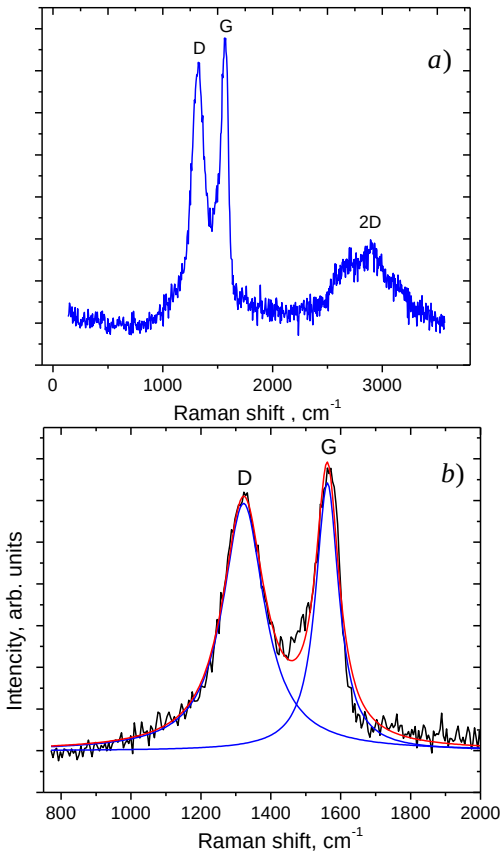

Fig. 2. (a) Raman spectra of graphite oxide/graphene oxide composite material and (b) D- and G-mode deconvolution results.

$L(nm) = (2.4 \times 10^{-10})\lambda^4 \left(\frac{I_D}{I_G}\right)$, where λ is the laser excitation wavelength. The observed D and G bands were fitted with two Lorentzian peaks (Fig.2, b). The average size of the graphite oxide packages L was 11.5 nm.

Summarizing the XRD and Raman results, we can propose the following model for the formation of a composite material. Synthesis conditions ensured local surface exfoliation of the original graphite particles. The exfoliation of the near-surface layers of the particles causes the formation of a graphite oxide fraction corresponding to Component 2 of the XRD pattern. At the same time, the dispergation of the initial particle leads to the formation of Component 1. The next oxidation of a small fragment of graphite oxide leads to the formation of colloidal graphene oxide.

SEM images (Fig. 3a) show highly wrinkled broken graphitic layers. The EDX maps (Fig. 3b–d) indicate the presence of carbon, oxygen, and sulfur on the surface of the samples, with sulfur being uniformly distributed both over the surface and along the edges of the lamellar particles of the material. Observed amount of elements: carbon –76.6 mass %, oxygen – 21.6 mass % and 1.8 mass %. The residual amount of sulfur in the range of 1.5 - 2 mass % is typical for graphene materials obtained by the Hummers method [15].

A study of the electrical properties of the resulting sulfur-doped graphene oxide/graphite oxide composite was carried out. Figure 4a shows current-voltage (I–V) curves with two prominent NDR regions observed along with an increase in current. Obtaining a differential curve allows one to clearly calculate the characteristics of the NDR signal, such as the peak voltage point (V_p), the valley voltage point (V_v), and also calculate the negative differential resistance $r_{diff} = \frac{[i(V_p) - i(V_v)]}{[V_p - V_v]}$. The results obtained are summarized in Table 1.

Table 1

Parameters of the NDR effect observed for the graphene oxide/graphite oxide composite material

V_p, V	V_v, V	i(V_p), mA	V_v, mA	r_{diff}
17.01	17.99	0.0865	0.0838	-0.0028

The electrical conductivity of the obtained graphene oxide/graphite oxide composite material is the result of a complex mutual influence of both mechanisms. The first is an electronic hopping between partially oxidized graphite particles forming a randomly distributed grid, and the second is a protonic mechanism of charge transport according to the Grotthuss mechanism [16].

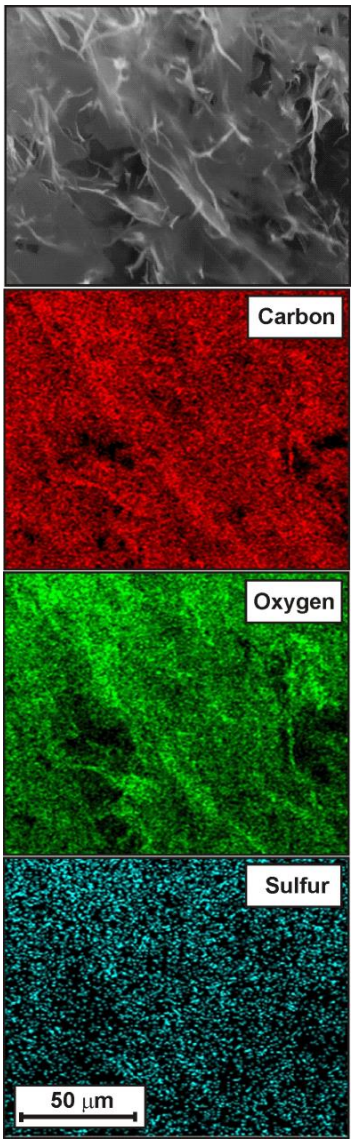

Fig. 3. (a) SEM image of the graphite oxide / graphene oxide composite material; EDX maps of the corresponding area for (b) carbon, (c) oxygen, and (d) sulfur.

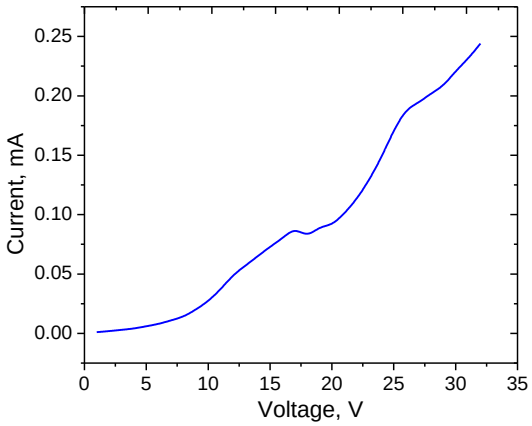

Fig. 4. I–V characteristics for a graphene oxide/graphite oxide composite with observation of a negative differential resistance.

Based on the synthesis conditions, it can be assumed that GO fragments are located between graphite oxide particles, and water molecules are embedded between graphene stacking layers [5]. The appearance of the NDR effect on the I–V characteristics of the conductivity of the graphene oxide/graphite oxide composite can be explained by H^+ hopping with reversible reduction of GO according to the following two-stage mechanism [10]:

$$H_2O \rightarrow 4H^+ + 4e^- + O_2 \quad \text{and} \quad GO + 2H^+ + 2e^- \rightarrow rGO + H_2O$$

An increase in the proton flow through the network of hydrogen bonds with an increase in the channel current is limited by the slow diffusion of adsorbed water molecules between hydrophilic functional groups (–OH, –COOH, and C–O–C) located on the surface of graphene layers. The imposition of these processes leads to the depletion of conduction channels and, thus, to NDR effects. It is clear that the magnitude of the NDR effect is determined by the fractions of functional groups immobilized on the GO surface and can be controlled by the synthesis conditions with an exact carbon-oxygen ratio. Doping with sulfur is an effective way to increase the GO conductivity due to its strong electron donor ability [17]. Sulfur atoms are preferably located at the sites of oxygen functional groups in GO, which contributes to a more efficient reduction process [18]. An increase in the electronic transport properties of S-doped GO as a component of the composite leads to an increase in the spatial separation of protons and electrons, as well as to an increase in the efficiency of the Grotthuss mechanism of charge transferring.

Conclusion

In this study, we have demonstrated a simple one-pot synthesis of sulfur doped graphite oxide / graphene oxide sheets as a promising functional material. The observation of negative differential resistance effect (NDR) in the current-voltage characteristics is due to a successful combination of the structural and electrical properties of materials consisting of a 3D grid of graphite oxide particles filled with interconnecting graphene oxide stacking layers. The proton hopping paths formed by water molecules adsorbed on the hydrophilic graphene layers are unstable due to thermal diffusion of these molecules, which causes depletion of the conduction channels and leads to the observation of NDR. The presence of sulfur atoms incorporated into the graphite oxide lattice most likely leads to an increase in the electronic conductivity and an increase in the NDR efficiency due to electron transfer to graphite oxide particles and increases the lifetime of H^+ transport ions.

Abaszade R.G. **–** Ass. Prof., Vice head of department "Electronics and automation";
Mamedov A.G. **–** Professor;
Bayramov I.Y. **-** Ass. Prof.;
Khanmamadova E.A. **-** Assistant;
Kotsyubynsky V.O. – Professor, Doctor of Physical and Mathematical Sciences;
Kapush O.A. **-** PhD, Senior Researcher, Department of Surface Physics and Semiconductor Nanophotonics;
Boychuk V.M. – Professor, Doctor of Physical and Mathematical Sciences;
Gür E.Y. – Professor, Department of Solid State Physics.

[1] F. Perrozzi, S. Prezioso, L. Ottaviano, Graphene oxide: From fundamentals to applications, *J. Phys. Condens. Matter.* 27, 013002 (2014); https://doi.org/10.1088/0953-8984/27/1/013002.
[2] V.M. Boychuk, V.O. Kotsyubunsky, K.V. Bandura, B.I. Rachii, I.P. Yaremiy, S.V. Fedorchenko, Structural and electrical properties of nickel-iron spinel/reduced graphene oxide nanocomposites, *Molecular Crystals and Liquid Crystals* 1(1), 137 (2019); https://doi.org/10.1080/15421406.2019.1578503.
[3] S. Vasileiadis, Z. Ziaka, Small scale reforming separation systems with nanomembrane reactors for direct fuel cell applications, *J. Nano R* 12, 105 (2010); https://doi.org/10.4028/www.scientific.net/JNanoR.12.105.
[4] J. Abraham, K.S. Vasu, C.D. Williams, K. Gopinadhan, Y. Su, C.T. Cherian, J. Dix, E. Prestat, S.J. Haigh, I.V. Grigorieva, P. Carbone, A.K. Geim, R.R. Nair, Tunable sieving of ions using graphene oxide membranes, *Nat. Nanotechnol.* 12, 546 (2017); https://doi.org/10.1038/nnano.2017.21.
[5] R.G. Abaszade, S.A. Mamedova, F.H. Agayev, S.I. Budzulyak, O.A. Kapush, M.A. Mamedova, A.M. Nabiyev, V.O. Kotsyubynsky, Synthesis and Characterization of Graphene Oxide Flakes for Transparent Thin Films, *Physics and Chemistry of Solid State* 22(3), 595 (2021); https://doi.org/10.15330/pcss.22.3.595-601.
[6] E. Aliyev, V. Filiz, M. M. Khan, Y. J. Lee, C. Abetz, V. Abetz, Structural characterization of graphene oxide: Surface functional groups and fractionated oxidative debris, Nanomaterials 9(8), 1180, (2019) https://doi.org/10.3390/nano9081180.

[7] S.R. Figarova, E.M. Aliyev, R.G. Abaszade, R.I. Alekberov, V.R. Figarov, Negative Differential Resistance of Graphene Oxide / Sulphur Compound, *Journal of Nano Research* 67, 25 (2021); https://doi.org/10.4028/www.scientific.net%2FJNanoR.67.25.
[8] S.R. Figarova, G.N. Hasiyeva, V.R. Figarov, Negative differential conductivity in quantum well with complex potential profile for electron–phonon scattering, *Physica E: Low-dimensional Systems and Nanostructures* 78, 10 (2016); http://dx.doi.org/10.1016/j.physe.2015.11.036.
[9] P. Sharma, L.S. Bernard, A. Bazigos, A. Magrez, A.M. Ionescu, Room-temperature negative differential resistance in graphene field effect transistors: experiments and theory, *ACS nano* 9(1), 620 (2015); https://doi.org/10.1021/nn5059437.
[10] S. Rathi, I. Lee, M. Kang, D. Lim, Y. Lee, S. Yamacli, G.H. Kim, Observation of negative differential resistance in mesoscopic graphene oxide devices, *Scientific reports* 8(1), 1 (2018); https://doi.org/10.1038/s41598-018-22355-0.
[11] I. Banerjee, P. Harris, A. Salimian, A.K. Ray, Graphene oxide thin films for resistive memory switches, *IET Circuits, Devices & Systems* 9(6), 428 (2015); https://doi.org/10.1049/iet-cds.2015.0170.
[12] E.M. Aliyev, M.M. Khan, A.M. Nabiyev, R.M. Alosmanov, I.A. Bunyad-zadeh, S. Shishatskiy, V. Filiz, Covalently Modified Graphene Oxide and Polymer of Intrinsic Microporosity (PIM- in Mixed Matrix Thin-Film Composite Membranes, *Nanoscale Research Letters* 13, 359 (2018); https://dx.doi.org/10.1186%2Fs11671-018-2771-3.
[13] L. Stobinski, B. Lesiak, A. Malolepszy, M. Mazurkiewicz, B. Mierzwa, J. Zemek, I. Bieloshapka, Graphene oxide and reduced graphene oxide studied by the XRD, TEM and electron spectroscopy methods, *Journal of Electron Spectroscopy and Related Phenomena* 195, 145 (2014); https://doi.org/10.1016/j.elspec.2014.07.003.
[14] M.A. Pimenta, G. Dresselhaus, M.S. Dresselhaus, L.G. Cancado, A. Jorio, R. Saito, *Physical chemistry chemical physics*, Studying disorder in graphite-based systems by Raman spectroscopy 9(11), 1276 (2007); https://doi.org/10.1039/B613962K.
[15] S. Drewniak, R. Muzyka, A. Stolarczyk, T. Pustelny, M. Kotyczka-Morańska, M. Setkiewicz, Studies of reduced graphene oxide and graphite oxide in the aspect of their possible application in gas sensors, *Sensors* 16(1), 103 (2016); https://doi.org/10.3390/s16010103.
[16] V.O. Kotsyubynsky, V.M. Boychuk, I.M. Budzulyak, B.I. Rachiy, M.A. Hodlevska, A.I. Kachmar, M.A. Hodlevsky, Graphene oxide synthesis using modified Tour method, *Advances in Natural Sciences: Nanoscience and Nanotechnology* 12(3), 035006 (2021); http://doi.org/10.1088/2043-6262/ac204f.
[17] Z. Tian, J. Li, G. Zhu, J. Lu, Y. Wang, Z. Shi, C. Xu, Facile synthesis of highly conductive sulfur-doped reduced graphene oxide sheets, *Physical Chemistry Chemical Physics* 18(2), 1125 (2016); https://doi.org/10.1039/C5CP05475C.
[18] Z. Wang, P. Li, Y. Chen, J. He, W. Zhang, O.G. Schmidt, Y. Li, Pure thiophene–sulfur doped reduced graphene oxide: synthesis, structure, and electrical properties, *Nanoscale* 6(13), 7281 (2014); https://doi.org/10.1039/C3NR05061K.

Р.Г. Абасзаде[1], А.Г. Мамедов [1], І.І. Байрамов[1], Е.А. Ханмамадова[1],
В.О. Коцюбинський[2], О.А. Капуш[3], В.М. Бойчук[2], Е.Ю. Гюр[4]

Структурні та електричні властивості допованого сіркою нанокомпозиту оксид графену / оксид графіту

[1]*Азербайджанський державний університет нафти і промисловості, Баку, Азербайджан, abaszada@gmail.com*
[2]*Vasyl Stefanyk Precarpathian National University, 57 Shevchenko str, Ivano-Frankivsk 76018, Ukraine. kotsuybynsky@gmail.com*
[3]*V.E. Lashkarev Institute of Semiconductor Physics, NASU, Kyiv, Ukraine, savchuk-olja@ukr.net*
[4]*Ataturk University, Erzurum 25240, Turkey, emregur@atauni.edu.tr*

Оригінальним шляхом було отримано легований сіркою нанокомпозитний матеріал оксид графену / оксид графіту. Здійснено детальне вивчення структурного впорядкування синтезованого композиту методами рентгеноструктурного аналізу та раманівської спектроскопії. Прояви явища негативного диференціального опору для отриманого матеріалу спостерігалися при кімнатній температурі було інтерпретовано в рамках моделі, яка передбачала просторово обмежений перколяційний транспорт протонів через молекули води, адсорбовані на гідрофільній поверхні шарів оксиду графену. Присутність збагаченого сіркою оксиду графіту з високою електронною провідністю сприяє просторовому розділенню протонів та електронів і підвищує ефективність перенесення H^+. Отримані результати відкривають можливості розробки нового способу синтезу композиційних матеріалів на основі графену з широким спектром практичних застосувань.

Ключові слова: оксид графену, оксид графіту, нанокомпозит, негативний диференціальний опір.